AIP | APL Materials
NOW INDEXED IN THOMSON REUTERS DATABASES

Research Update: Atmospheric pressure spatial atomic layer deposition of ZnO thin films: Reactors, doping, and devices

Robert L. Z. Hoye, David Muñoz-Rojas, Shelby F. Nelson, Andrea Illiberi, Paul Poodt, Fred Roozeboom, and Judith L. MacManus-Driscoll

Citation: APL Materials **3**, 040701 (2015); doi: 10.1063/1.4916525
View online: http://dx.doi.org/10.1063/1.4916525
View Table of Contents: http://scitation.aip.org/content/aip/journal/aplmater/3/4?ver=pdfcov
Published by the AIP Publishing

Articles you may be interested in
Effect of Al concentration on Al-doped ZnO channels fabricated by atomic-layer deposition for top-gate oxide thin-film transistor applications
J. Vac. Sci. Technol. B **32**, 041202 (2014); 10.1116/1.4880823

Influence of aluminium doping on thermoelectric performance of atomic layer deposited ZnO thin films
Appl. Phys. Lett. **103**, 203903 (2013); 10.1063/1.4831980

Atomic layer deposition of Al-doped ZnO thin films
J. Vac. Sci. Technol. A **31**, 01A109 (2013); 10.1116/1.4757764

Low temperature atomic layer deposited Al-doped ZnO thin films and associated semiconducting properties
J. Vac. Sci. Technol. B **30**, 031210 (2012); 10.1116/1.4710519

Growth morphology and electrical/optical properties of Al-doped ZnO thin films grown by atomic layer deposition
J. Vac. Sci. Technol. A **30**, 021202 (2012); 10.1116/1.3687939

Did your publisher get
18 MILLION DOWNLOADS in 2014?
AIP Publishing did.

THERE'S POWER IN NUMBERS. Reach the world with AIP Publishing.

This article is copyrighted as indicated in the article. Reuse of AIP content is subject to the terms at: http://aplmaterials.aip.org/about/rights_and_permissions
Downloaded to IP: 131.111.184.102 On: Mon, 01 Jun 2015 10:48:06

APL MATERIALS 3, 040701 (2015)

Research Update: Atmospheric pressure spatial atomic layer deposition of ZnO thin films: Reactors, doping, and devices

Robert L. Z. Hoye,[1,a] David Muñoz-Rojas,[2] Shelby F. Nelson,[3] Andrea Illiberi,[4] Paul Poodt,[4] Fred Roozeboom,[4,5] and Judith L. MacManus-Driscoll[1,a]
[1]*Department of Materials Science and Metallurgy, University of Cambridge, 27 Charles Babbage Road, Cambridge CB3 0FS, United Kingdom*
[2]*LMGP, University Grenoble-Alpes, CNRS, F-3800 Grenoble, France*
[3]*Kodak Research Laboratories, Eastman Kodak Company, Rochester, New York 14650, USA*
[4]*Holst Centre/TNO Thin Film Technology, Eindhoven, 5656 AE, The Netherlands*
[5]*Department of Applied Physics, Eindhoven University of Technology, P.O. Box 513, Eindhoven, 5600 MB, The Netherlands*

(Received 31 December 2014; accepted 17 March 2015; published online 2 April 2015)

Atmospheric pressure spatial atomic layer deposition (AP-SALD) has recently emerged as an appealing technique for rapidly producing high quality oxides. Here, we focus on the use of AP-SALD to deposit functional ZnO thin films, particularly on the reactors used, the film properties, and the dopants that have been studied. We highlight how these films are advantageous for the performance of solar cells, organometal halide perovskite light emitting diodes, and thin-film transistors. Future AP-SALD technology will enable the commercial processing of thin films over large areas on a sheet-to-sheet and roll-to-roll basis, with new reactor designs emerging for flexible plastic and paper electronics. © *2015 Author(s). All article content, except where otherwise noted, is licensed under a Creative Commons Attribution 3.0 Unported License.* [http://dx.doi.org/10.1063/1.4916525]

I. INTRODUCTION: ATMOSPHERIC PRESSURE SPATIAL ATOMIC LAYER DEPOSITION (AP-SALD)

The recent boom of nanoscience and nanotechnology,[1,2] particularly for the miniaturization and diversification of electronics,[3] has prompted the need for semiconductor fabrication techniques that can rapidly produce high quality thin films in a scalable, controlled manner with tunable electrical properties.[4] Atmospheric pressure spatial atomic layer deposition (AP-SALD) is an emerging technique to produce functional oxides, such as ZnO, for devices.[5] AP-SALD has the capability of rapid, atmospheric and in-line processing in industrial environments.[5–7] Spatial atomic layer deposition (SALD) evolved from conventional atomic layer deposition (ALD) to overcome the limitations of ALD in a vacuum environment: although ALD can controllably produce conformal, pinhole-free thin films,[5,6,8–13] long purge steps are needed between the alternating precursor exposure steps to prevent their intermixing in the gas phase and to ensure that they are separately chemisorbed onto the substrate (Fig. 1(a)). This limits its growth rate to typically $\sim 10^{-2}$–10^{-1} nm s^{-1}.[6,8,12,14,15] In SALD processes, by contrast, the precursors are separated spatially (hence *spatial* ALD) and the substrate moves between the different precursor zones (Fig. 1(b)).[16] While some SALD reactors operate at low pressures in a closed chamber, most SALD reactors are designed to operate at atmospheric pressure.[6] It is these AP-SALD reactors that we will focus on in this research update. We specifically focus on AP-SALD reactors because avoiding closed chamber or vacuum based steps

[a]Authors to whom correspondence should be addressed. Electronic addresses: rlzh2@cam.ac.uk and jld35@cam.ac.uk, Telephone: +44 (0) 1223 334 468.

 ©Author(s) 2015

This article is copyrighted as indicated in the article. Reuse of AIP content is subject to the terms at: http://aplmaterials.aip.org/about/rights_and_permissions Downloaded to IP: 131.111.184.102 On: Mon, 01 Jun 2015 10:48:06

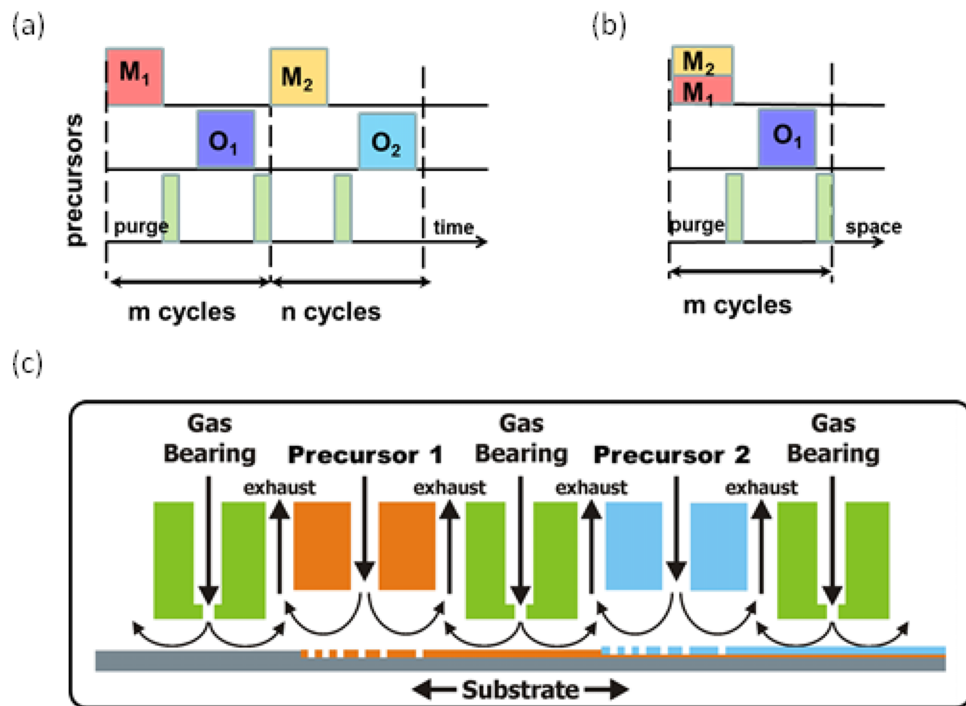

FIG. 1. Illustration of the production of doped metal oxides by (a) delta-doping using conventional ALD and (b) co-injection using AP-SALD.[31] (c) Schematic of an example AP-SALD gas manifold, showing how the separate gas channels are created, with the precursor channels spatially separated by inert gas channels that can also act as gas bearings to float the manifold over the substrate (or vice versa).[30]

in device synthesis is highly preferable for their industrial application.[5,14,17,18] Detailed reviews of closed chamber and atmospheric pressure spatial ALD reactors and their development can be found in Refs. 5 and 6.

In the few years that AP-SALD has now been in development, ZnO has received much attention, since it is a non-toxic metal oxide with widely varying properties depending on doping (e.g., with Mg, N, Al, or In).[13,19–21] ZnO is also an earth-abundant material, has a wide bandgap, and can be processed over large areas, making it suitable for next generation electronics, such as smart window layers, nanorod arrays, and transparent conductors in thin-film solar cells and as switching channels in thin-film transistor (TFT) circuits.[13,19,20,22] Producing ZnO by AP-SALD is very appealing because the high throughput of this technique makes it suitable for devices requiring high production rates, such as in excitonic solar cells.[22–24] Furthermore, the use of AP-SALD to control and tune the electronic properties of ZnO through doping is now recognized as a low-cost and scalable way to increase the performance of these devices.[19,20,25] The controlled introduction of dopants by AP-SALD is an important challenge, and the recent progress made for a narrow group of dopants could pave the way for future developments, as the interest in AP-SALD and range of dopants used becomes broader to the level achieved with doped ZnO deposited by conventional ALD.[13]

This research update focuses on the deposition of functional ZnO films using AP-SALD. It starts by discussing the main AP-SALD reactor designs that have been used to synthesize ZnO at atmospheric pressure. We also seek to standardize the terminology used. For example, the various terms previously employed to describe these reactors are atmospheric atomic layer deposition (AALD),[23–26] spatial atmospheric atomic layer deposition (SAALD),[5,27,28] and atmospheric spatial atomic layer deposition.[29] Here, the term is standardized to AP-SALD. AP-SALD reactors have also previously been simply termed "spatial atomic layer deposition" (S-ALD or SALD).[16,30,31] But as noted above, some SALD reactors operate in a closed chamber, whereas we are most interested in those that operate at atmospheric pressure. In Sec. II, we discuss the methods of doping and effects

This article is copyrighted as indicated in the article. Reuse of AIP content is subject to the terms at: http://aplmaterials.aip.org/about/rights_and_permissions
Downloaded to IP: 131.111.184.102 On: Mon, 01 Jun 2015 10:48:06

of dopants on properties. We then highlight the influence of intrinsic and doped AP-SALD ZnO films on thin-film solar cells, organometal halide perovskite light emitting diodes (PeLEDs) and transistors. In particular, we highlight the advantages of using ZnO synthesized by AP-SALD, as well as the necessary future developments that must be undertaken.

II. AP-SALD REACTOR DESIGNS

In AP-SALD, inert gas curtains are used to spatially separate the precursor gases, thus keeping them chemically isolated (Fig. 1(c)).[5,6,16,27,31] The isolation of each gas channel is also maintained by positioning the substrate <100 nm from the gas manifold and ensuring that the exhaust flow of gases balances the inlet gas flow.[31] The substrate position may be maintained by mechanically constraining the gas manifold over the substrate,[25] floating the gas manifold over the substrate (where the gas curtains act as frictionless bearings),[32] or by floating the substrate over the gas manifold.[31] It is important to avoid gas intermixing, since this results in chemical vapor deposition (CVD).[33,34] Inert carrier gas (e.g., N_2) is bubbled through the liquid organometallic metal precursor(s) and oxidant (H_2O). The vapors of the metal precursor(s), oxidant, and the inert gas are separately fed to the gas manifold. The gas manifold divides and guides the gas flows in such a way that there is an inert gas channel between each precursor (metal or oxidant) channel (Fig. 1(c)). By moving the substrate along these curtains, a much faster ALD cycle (metal precursor exposure/purge/oxidant exposure/purge) is replicated. This reactant alternation principle allows AP-SALD to grow metal oxide films monolayer by monolayer up to two orders of magnitude faster (in nm s^{-1}) than conventional ALD.[23,24,35] Since AP-SALD replicates the ALD cycles and reactions, the advantages of ALD processing are maintained: atomic-level thickness control,[32] and high quality, pinhole-free films with controllable properties.[23,25,26,36] This also results in the growth rate in nm $cycle^{-1}$ being similar for conventional ALD and AP-SALD (Table I). AP-SALD also uses the same deposition temperatures as ALD (often ~150 °C for ZnO), since the chemical half-reactions involved are the same.[23,25,26,36] The low temperatures are compatible with some industrial polymer substrates, which for AP-SALD enable the process to be compatible with atmospheric pressure, roll-to-roll (R2R) deposition of ZnO onto continuous substrates (e.g., polymers, foil, or paper).[23,34,37,38]

AP-SALD ZnO was first reported by Levy *et al.*[16] Their reactor was further developed by Cambridge University and used to produce Cu_2O,[35] TiO_2,[24] and doped and intrinsic ZnO.[18,23,25,26,28,36,39] Various names have been given to describe this system, but in this research update, we standardize its name to the Cambridge University Close Proximity (CUCP) reactor (design details are given in Ref. 24). An illustration of the CUCP gas manifold is given in Fig. 2. In this reactor, gas isolation is achieved by mechanically constraining the manifold <50 μm above the substrate and balancing the inlet and exhaust gas flows.[24] One limitation of this design is that the manifold-substrate spacing is sometimes too high (since it is mechanically constrained), and the pressure gradient for each gas channel is insufficient to maintain gas isolation. This results in precursor gas intermixing and the films depositing by AP-CVD.[31] However, we have found that the AP-CVD films remain strongly

TABLE I. Comparison of the deposition conditions and parameters for intrinsic ZnO grown using conventional ALD vs. AP-SALD reactors.

Reactor	Deposition temperature (°C)	Growth rate (nm s^{-1})	Growth rate (nm $cycle^{-1}$)	Sample size	Reference
		Conventional ALD			
(Microchemistry F-120)	105–180	0.13–0.18	0.15–0.21	⋯	15
		AP-SALD			
CUCP	150	0.63	0.25	3.5×5.5 cm[a]	23
Kodak[b]	100–250	0.05–2	0.15–0.23	2.5×5 cm	9, 40
TNO	75–250	0.3–0.9	0.18	3 cm wide ring[c]	5, 30
SoLayTec InPassionLAB	100–260	0.29–0.61	0.09–0.19	156×156 mm	42

[a]The sample size can be adjusted by changing the length of linear oscillation of the substrate beneath the gas manifold.[23,24]
[b]Kodak refers to the head designed by the Eastman Kodak Company.
[c]The substrate holder is a 3 cm wide ring, on which any sized substrate can be loaded.[32]

This article is copyrighted as indicated in the article. Reuse of AIP content is subject to the terms at: http://aplmaterials.aip.org/about/rights_and_permissions Downloaded to IP: 131.111.184.102 On: Mon, 01 Jun 2015 10:48:06

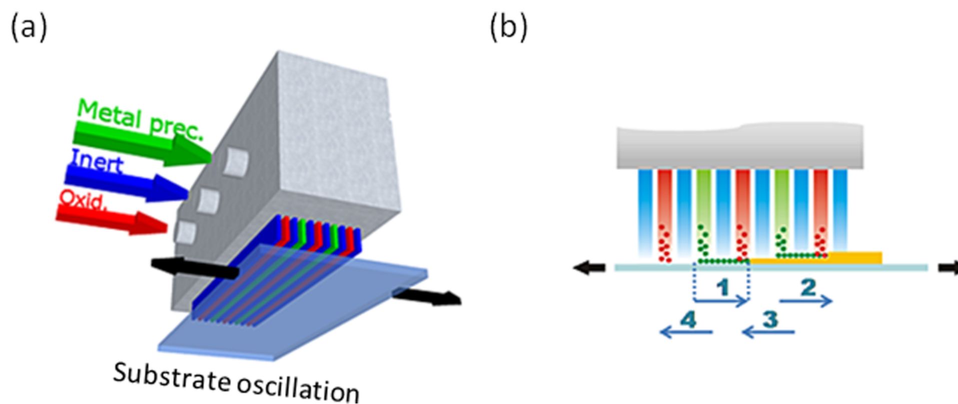

FIG. 2. Illustration of the CUCP reactor. (a) CUCP gas manifold. The metal precursor, inert gas, and oxidant gases are introduced to separate inlets and guided to one side of manifold. They travel through horizontal channels beneath the manifold across to the exhaust on the other side. The substrate oscillates beneath these gas channels to grow the metal oxide film, as schematically illustrated in (b). The substrate moves through the metal precursor channel (green), where the metal precursor chemisorbs to the substrate. Next, the substrate moves through an inert channel (blue) to the oxidant channel (red) to form a monolayer of the oxide. In one cycle, the substrate moves under a metal precursor channel four times, as indicated. Reprinted with permission from D. Muñoz-Rojas, H. Sun, D. C. Iza, J. Weickert, L. Chen, H. Wang, L. Schmidt-Mende, J. L. MacManus-Driscoll, Prog. Photovoltaics: Res. Appl. **21**, 393 (2013). Copyright 2013 Wiley-VCH.

adherent to the substrate, compact, pinhole-free as-deposited with similar carrier properties, grain structure, crystallinity, and transmittance as ALD films. We can also control the film thickness through the number of cycles. The main difference is that we obtain a higher growth rate when using our system as an AP-CVD reactor rather than as an AP-SALD reactor. The disadvantage of operating the CUCP reactor in AP-CVD mode is that the films are often thicker on the inlet side of the manifold and thinner on the exhaust side of the manifold. This is due to the concentration of precursors being lower at the exhaust due to reaction upstream of the gas channels. Avoiding this thickness variation can be achieved by having an optimized design with the inlet gas introduced via a channel running along the length of the manifold and having the exhaust channels immediately adjacent to each inlet channel.

In 2009, a different head designed by the Eastman Kodak Company was reported, in which the substrate floats over the gas channels (details in Ref. 31 and illustrated in Figs. 3(a) and 3(b)). Unlike the CUCP reactor, this design results in a small substrate-manifold spacing (∼17 μm), creating a large and well-defined pressure field that provides a large driving force for the inlet gas to flow to their adjacent exhaust channels. The AP-SALD head designed by the Eastman Kodak Company also has the exhaust channels immediately adjacent to the inlet channels, unlike the CUCP design.[16,24,31] In addition to balancing the inlet and exhaust gas flow rates, these factors make the head designed by the Eastman Kodak Company extremely effective at maintaining gas isolation.[31] By controlling the substrate velocity, rapid ALD synthesis of ZnO can occur (up to 2 nm s^{-1}), which is an order of magnitude higher than the growth rate of conventional ALD (Table I).[9,14,40] The range in growth rates shown is due to this parameter being a function of deposition temperature and residence time, which is controlled by pulse duration (conventional ALD)[15] or substrate velocity (AP-SALD).[9,40] In Table I, the growth rate of 2 nm s^{-1} using the AP-SALD head designed by the Eastman Kodak Company was obtained using an exposure time of 25 ms (100 ms for each cycle) at 200 °C.[40]

A similar design was developed by TNO (Fig. 3(c)),[32] in which the gas manifold is floated ∼20 μm over the substrate (Fig. 1(c)), as detailed in Refs. 6, 30, and 32. As with the AP-SALD head designed by the Eastman Kodak Company, gas isolation is maintained by balancing the inlet and exhaust flow rates and having a large inert gas bearing between the precursor inlets.[32,41] The substrate is rotated at up to 3000 rpm, leading to deposition rates almost reaching 1 nm s^{-1} for ZnO (Table I) and 3–4 nm s^{-1} for Al_2O_3.[30,32] The deposition rate of AP-SALD is thus only limited by reaction rates for planar, featureless substrates, and maintaining an ALD growth regime (rather than a CVD growth regime) leads to uniform films to be deposited.[32]

This article is copyrighted as indicated in the article. Reuse of AIP content is subject to the terms at: http://aplmaterials.aip.org/about/rights_and_permissions
Downloaded to IP: 131.111.184.102 On: Mon, 01 Jun 2015 10:48:06

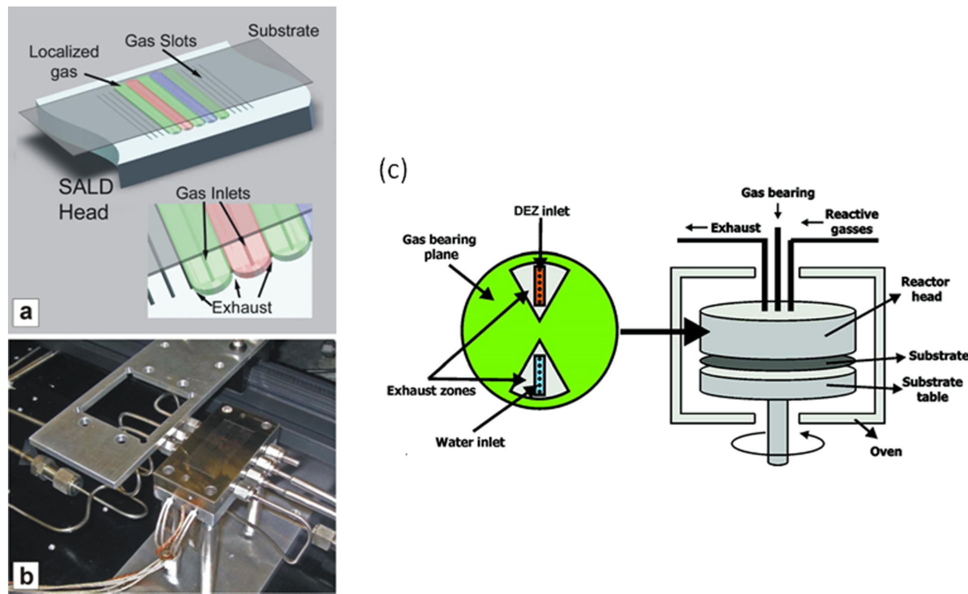

FIG. 3. Illustration of AP-SALD reactors based on gas bearings. (a) Illustration of substrate floating over the head designed by the Eastman Kodak Company, a photograph of which is shown in (b). Reprinted with permission from P. Poodt, D. C. Cameron, E. Dickey, S. M. George, V. Kuznetsov, G. N. Parsons, F. Roozeboom, G. Sundaram, A. Vermeer, J. Vac. Sci. Technol. A **30**, 010802 (2012). Copyright 2012 AIP Publishing LLC. (c) Illustration of the TNO reactor with a view of underneath the gas manifold, showing the gas zones. Reprinted with permission from A. Illiberi, R. Scherpenborg, Y. Wu, F. Roozeboom, P. Poodt, ACS Appl. Mater. Interfaces **5**, 13124 (2013). Copyright 2013 American Chemical Society.

Other AP-SALD reactors have been produced, but they have mainly been reported to synthesize Al_2O_3 films.[6,43] These reactors can, however, also produce intrinsic and doped ZnO films using the reactants and concepts we highlight in this research update. One such industrial AP-SALD reactor is that offered by SoLayTec. This uses gas bearings and operates in a similar fashion to the TNO AP-SALD (details in Ref. 6). While most early publications with the SoLayTec reactors have focused on Al_2O_3,[6] a recent publication details studies into ZnO.[42] The deposition conditions and growth rates are shown in Table I.

III. AP-SALD OF INTRINSIC AND DOPED ZNO: SYNTHESIS AND DEVICES

In both conventional ALD and AP-SALD of intrinsic ZnO, diethylzinc (DEZ) vapor is used as the Zn precursor and water vapor as the oxygen source.[15,23,30,31] From Figure 4, it can be seen that AP-SALD ZnO deposited at 150 °C using diethylzinc and water as the precursors has a grain size of

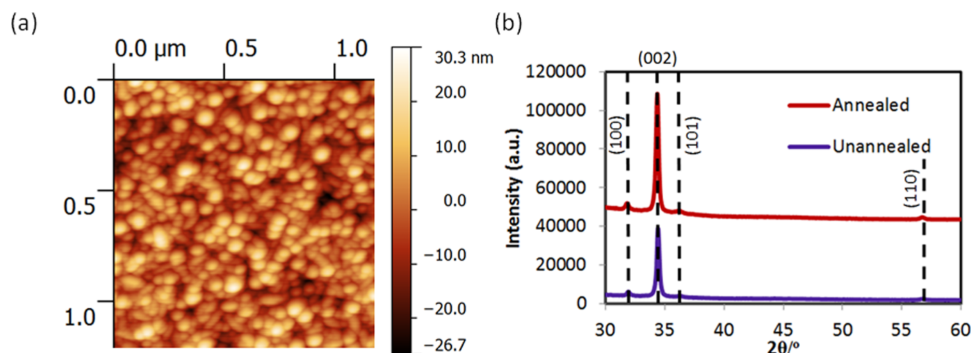

FIG. 4. Morphology of AP-SALD ZnO films synthesized using the CUCP reactor. (a) Atomic force microscopy (AFM) topography image of unannealed ZnO and (b) X-ray diffraction (XRD) patterns of unannealed and annealed (at 300 °C for 1 h) ZnO. The deposition temperature was also 150 °C and the films ~100 nm thick.[23]

This article is copyrighted as indicated in the article. Reuse of AIP content is subject to the terms at: http://aplmaterials.aip.org/about/rights_and_permissions Downloaded to IP: 131.111.184.102 On: Mon, 01 Jun 2015 10:48:06

~50 nm (Fig. 4(a)), strong c-axis orientation, and high crystallinity (Fig. 4(b)). These properties are the same as those of ZnO synthesized by conventional ALD, as can be seen from Figures 2(a) and 4 in Ref. 44.

One important application of ZnO is in thin-film solar cell production, such as those based on polymers or organometal halide perovskites, which have gained increasing attention as a low-cost alternative to silicon solar cells.[45,46] AP-SALD ZnO could be used as the semiconductor in TFTs.[9,20,40,41,47,48] This is particularly important because TFTs (acting as a switch) have become a crucial part of the electronics industry, especially for displays. Several million TFTs are produced each year for displays.[49] When ZnO was used in TFTs, the source and drain contacts could be placed on it.[31] For example, Ref. 31 shows a TFT structure with a chromium gate, AP-SALD Al_2O_3 dielectric, AP-SALD ZnO semiconductor and aluminum source, and drain contacts on top of the ZnO.

In order to expand the potential of AP-SALD, multicomponent ZnO-based materials have been developed through doping ZnO by AP-SALD. Doping is essential for tailoring and optimizing the electronic and optical properties of ZnO.[19] Here, we consider the important properties of ZnO that have been tuned for a variety of device applications.

A. ZnO conduction band tuning

The conduction band position of ZnO is important for controlling interfacial recombination in solar cells, as well as the turn-on voltage in light emitting diodes (LEDs).[11,18,19,25,28,39,50] A particularly effective way of tuning the ZnO conduction band position is through Mg incorporation.[51] This has been achieved by AP-SALD using bis(ethylcyclopentadienyl)magnesium ($Mg(CpEt)_2$) as the magnesium precursor.[25] Inert gas was bubbled through each organometallic precursor and these gases, saturated with the precursor, were mixed in the pipeline before being fed to the manifold (detailed in Ref. 25). This is known as the *co-injection* method, where the metal precursors are mixed in the gas phase and introduced to the reactor in the same gas stream (Fig. 1(b)). One distinct limitation of using this method for the $Zn_{1-x}Mg_xO$ precursors is that the Mg precursor has a lower vapor pressure than the Zn precursor (DEZ), resulting in low Mg incorporation.[25] To increase the fraction of $Mg(CpEt)_2$ in the gas phase, the bubbling rate through the Mg precursor had to be more

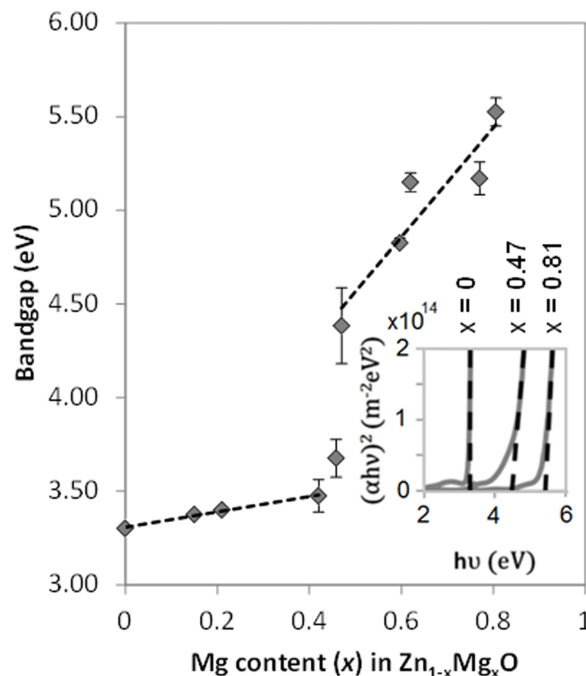

FIG. 5. Change in ZnO bandgap with the amount of Mg incorporated.[25]

This article is copyrighted as indicated in the article. Reuse of AIP content is subject to the terms at: http://aplmaterials.aip.org/about/rights_and_permissions Downloaded to IP: 131.111.184.102 On: Mon, 01 Jun 2015 10:48:06

than 25 times higher than the bubbling rate through the Zn precursor, and while the DEZ was kept at room temperature, the Mg precursor was heated to 55 °C to increase its vapor pressure. Up to 81 at. %, Mg was thus incorporated into ZnO, resulting in a bandgap increase from 3.3 eV (intrinsic ZnO) to 5.5 eV (81 at. % Mg in ZnO), as shown in Fig. 5.[25] This is more than that achievable by metal-organic chemical vapor deposition[33] and comparable to that achieved using high-quality vacuum-based processes, such as pulsed laser deposition.[52]

AP-SALD $Zn_{1-x}Mg_xO$ has also been used to study open-circuit voltage (V_{OC}) loss mechanisms in depleted-heterojunction colloidal quantum dot solar cells (DH-CQDSCs, see Refs. 53 and 54). In even the most efficient solar cells of this type, the V_{OC} values are well below theoretical limits.[55] By tuning the ZnO conduction band position through incorporating Mg into ZnO (thus forming $Zn_{1-x}Mg_xO$–PbSe CQDSCs), the amount of electron thermalization via the metal oxide band-tail (Fig. 6(a)) was reduced, leading to the V_{OC} values being increased from 408 mV to 608 mV, the highest for PbSe DH-CQDSCs at the time of publication. This work shows that more efficient CQDSCs can be obtained by using new electron acceptors without a pronounced conduction band tail and with an electron acceptor level at the same position as the quantum dot conduction band.[25] Another loss mechanism is interfacial recombination, which is when electrons injected from the p-type absorber into the n-type layer (e.g., ZnO) tunnel back to recombine with a hole either in the p-type layer or at the interface.[26] Interfacial recombination is enhanced when the conduction band of the n-type material is deeper than the conduction band of the p-type layer (cliff),[11] as illustrated in Fig. 6(b) for cuprous oxide (Cu_2O) solar cells.[28] Reducing this conduction band offset through

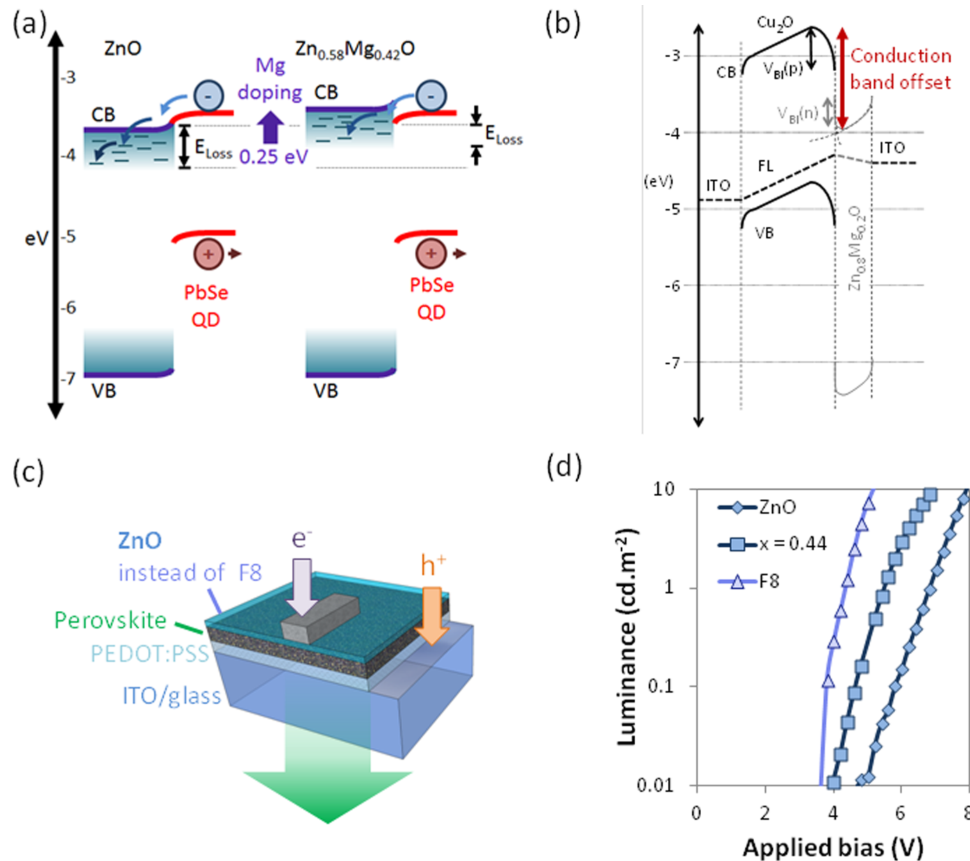

FIG. 6. The beneficial properties of AP-SALD zinc magnesium oxide ($Zn_{1-x}Mg_xO$) for optoelectronics. (a) Illustration of how raising the ZnO conduction band tail through Mg incorporation reduces open-circuit voltage losses in PbSe quantum dot solar cells due to electron-thermalization via metal oxide band-tails.[25] (b) Illustration of the conduction band offset between Cu_2O and $Zn_{0.8}Mg_{0.2}O$ in Cu_2O heterojunction thin-film solar cells.[28] (c) Structure of $CH_3NH_3PbBr_3$ PeLEDs with $Zn_{1-x}Mg_xO$ electron-injectors.[39] (d) Reduction in turn-on voltage (on luminance vs. applied bias plot) of PeLEDs by incorporating Mg into the ZnO electron-injector, compared with PeLEDs with F8 as the electron-injector.[39]

This article is copyrighted as indicated in the article. Reuse of AIP content is subject to the terms at: http://aplmaterials.aip.org/about/rights_and_permissions
Downloaded to IP: 131.111.184.102 On: Mon, 01 Jun 2015 10:48:06

Mg incorporation into the ZnO layer, therefore, reduces interfacial recombination, giving high V_{OC} values and efficiencies.[28] Further improvements, however, will depend on avoiding forming the more stable CuO phase on Cu_2O when it is heated atmospherically during the deposition of AP-SALD $Zn_{1-x}Mg_xO$ on top.[7]

$Zn_{1-x}Mg_xO$ has also been studied in LEDs (see Ref. 56 for working principles) and using the CUCP reactor, the metal oxide has been directly deposited onto methylammonium lead tribromide perovskites ($CH_3NH_3PbBr_3$), producing PeLEDs (Fig 6(c)) with sharp electroluminescence (peak full width half maximum of only 25 nm).[39] Since these organometal halide perovskites are heat sensitive, deposition of the electron-injection layer at more than 100 °C produces an increase in the pore size in the $CH_3NH_3PbBr_3$ layer, which leads to shunting. The advantage of AP-SALD is that the processing time of the oxide is minimized: the deposition does not occur in a vacuum-chamber and so the organometal halide perovskite sample can be directly loaded and unloaded from the substrate holder.[39] ZnO conduction band tuning by Mg incorporation allows the electron-injection barrier to be reduced when the ZnO electron-affinity is reduced. This results in a reduction in the turn-on voltages to a comparable level as PeLEDs using F8 (poly(9,9-dioctylfluorene)) as the electron-injector (Fig. 6(d), Table II). Use of $Zn_{1-x}Mg_xO$ instead of F8 also has the distinct advantage of ensuring luminescence is only from the organometal halide perovskite.[39]

TABLE II. Deposition conditions for producing doped ZnO by AP-SALD and the effects of the dopants on the materials properties and in devices.

Dopant	Dopant precursor	Reactor	Deposition temperature (°C)	Growth rate (nm s^{-1})	Main effect in ZnO films; devices	Reference
Mg	$Mg(CpEt)_2$[a]	CUCP	150	0.28	Raises ZnO conduction band; increases V_{OC} in PbSe quantum dot solar cells	25
Mg	$Mg(CpEt)_2$	CUCP	80–100	0.29–0.36	Raises ZnO conduction band; increases V_{OC} in Cu_2O solar cells	18, 28
Mg	$Mg(CpEt)_2$	CUCP	60	0.17	Raises ZnO conduction band; reduces turn-on voltage in LEDs by reducing electron-injection barrier	39
N	$NH_{3(aq)}$[a]	CUCP	150	0.36	Reduces carrier concentration of ZnO from ~10^{19} cm^{-3} (intrinsic) to ~10^{17} cm^{-3} (0.22 at. % N) and increases resistivity from 0.4 Ω cm to 160 Ω cm; reduces interfacial recombination and increases exciton dissociation at hybrid interfaces	26, 36
N	$NH_{3(aq)}$	CUCP	150	0.36	Produces p-type ZnO with post-deposition treatment	16, 57
N	$NH_{3(aq)}$	Kodak	200	0.9–1.8	Increases ZnO resistance by over an order of magnitude; improves TFT gating with sharp transistor turn-on	9, 20
Al	TMA[a]	TNO	200	0.20–0.33	Reduces ZnO resistivity from 0.1 Ω cm to 2×10^{-3} Ω cm, with a transmittance of 90%	5, 27
Al	DMAI[a]	Kodak	100–300	0.5–1.5[b]	Reduces ZnO resistivity from ~7×10^{-3} Ω cm to 4.56×10^{-4} Ω cm	9, 40
In	TMIn[a]	TNO	200	0.28	Reduces the ZnO resistivity from 5 Ω cm to 3×10^{-3} Ω cm, with 90% transmittance	29

[a]Abbreviations: $Mg(CpEt)_2$ is bis(ethylcyclopentadienyl)magnesium, $NH_{3(aq)}$ is ammonia in aqueous solution, TMA is trimethyl aluminium, DMAI is dimethylaluminium isopropoxide, TMIn is trimethyl indium, and TFT is thin-film transistor.
[b]The highest growth rate of 1.5 nm s^{-1} (0.15 nm $cycle^{-1}$ with a residence time of 25 ms) was obtained at a deposition temperature of 200 °C.[40]

This article is copyrighted as indicated in the article. Reuse of AIP content is subject to the terms at: http://aplmaterials.aip.org/about/rights_and_permissions Downloaded to IP: 131.111.184.102 On: Mon, 01 Jun 2015 10:48:06

B. ZnO carrier property tuning

For optimizing the properties of solar cells, thin-film transistors, and transparent conducting oxides (TCOs), which all rely on ZnO thin films, careful control of the carrier concentrations is required.[9,26,27,29,36,40] Nitrogen-doping of ZnO reduces its carrier concentration (thus increasing resistivity, as shown in Table II),[9,26] and it has been claimed that it can make ZnO p-type with post-deposition treatment (Table II).[26,57] The nitrogen dopant is introduced by mixing ammonia with the water oxidant precursor, and this is the method used for both conventional and spatial ALD ZnO:N.[26,58] The non-pyrophoric and low-cost nature of the ammonia precursor is in contrast to the expensive, pyrophoric organometallic materials that are often used as ALD and AP-SALD precursors,[5,14] and hence ammonia has been widely studied in both ALD and AP-SALD ZnO.[26,36,57–59] It is suspected that nitrogen doping reduces the carrier concentration because it is an acceptor dopant that compensates the intrinsic donors.[26,57]

In ZnO–PbS DH-CQDSCs, doping the ZnO with nitrogen has been shown to reduce interfacial recombination (Fig. 7(a)). Studies have indicated that this is due to a reduction in the back transfer of electrons or by enabling greater collection of electrons in PbS quantum dot intragap states to sub-bandgap states in the ZnO, as the ZnO carrier concentration is reduced.[26] In TFTs, if the ZnO carrier concentration is too high, then there is a high drain current in the "off" state. Reducing the carrier concentration through nitrogen-doping (by either conventional or spatial ALD) has been found to lower off-currents, showing this doping technique to be an important tool for improving TFT performance.[9,58]

While ZnO:N films can be produced by AP-SALD and conventional ALD from the same reactants, an important advantage of AP-SALD is that it is easier to achieve short exposure times (<100 ms), since fast substrate speeds and narrow gas channels are used.[9,16] An important consequence of shorter pulse times is that the resistance of ZnO increases with decreasing pulse times. By using a shorter purge time after DEZ precursor exposure, there may be less precursor decomposition and an increase in resistivity. Consistent with that, it is well known that ALD ZnO films grown at lower temperatures (which would have less precursor decomposition) are more resistive.[9]

Whereas nitrogen-doping reduces the carrier concentration of ZnO, doping ZnO with Al and In increases its carrier concentration because these group III cationic substituents have a higher valence than Zn^{2+} and are electron donors that raise the ZnO Fermi level to or beyond its conduction band (making the ZnO degenerate) to produce a TCO.[19] Unlike nitrogen-doping, both Al and In require organometallic precursors, such as trimethyl aluminum (TMA) or dimethyl aluminum isopropoxide (DMAI) for Al, and trimethyl indium (TMIn) for In, as shown in Table II.[14,27,29,40,60,61]

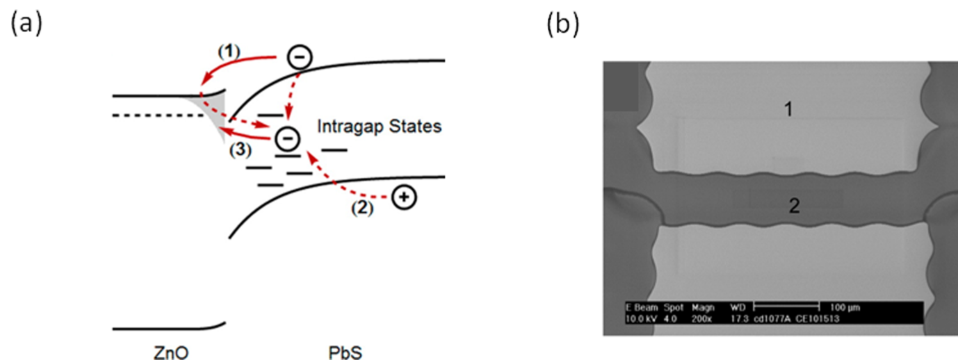

FIG. 7. (a) Band-diagram of ZnO–PbS quantum dot solar cells, showing how electrons injected into ZnO can undergo recombination via trap states at the interface. This figure differs from Fig. 6(a) because smaller bandgap (1.03 eV) PbS quantum dots (rather than 1.43 eV bandgap PbSe quantum dots) are illustrated, and focuses on interfacial recombination processes. Reprinted with permission from B. Ehrler, K. P. Musselman, M. L. Böhm, F. S. F. Morgenstern, Y. Vaynzof, B. J. Walker, J. L. MacManus-Driscoll and N. C. Greenham, ACS Nano **7**, 4210 (2013). Copyright 2013 American Chemical Society. (b) SEM image of patterned AP-SALD metal oxide films (Al-doped ZnO or AZO in this case) using a water-soluble poly(vinyl pyrrolidone) or PVP inhibitor. Region 1 (light gray) is 100 nm thick AZO and region 2 (dark gray) is PVP. Reprinted with permission from C. Ellinger and S. F. Nelson, Chem. Mater. **26**, 1514 (2014). Copyright 2014 American Chemical Society.

This article is copyrighted as indicated in the article. Reuse of AIP content is subject to the terms at: http://aplmaterials.aip.org/about/rights_and_permissions Downloaded to IP: 131.111.184.102 On: Mon, 01 Jun 2015 10:48:06

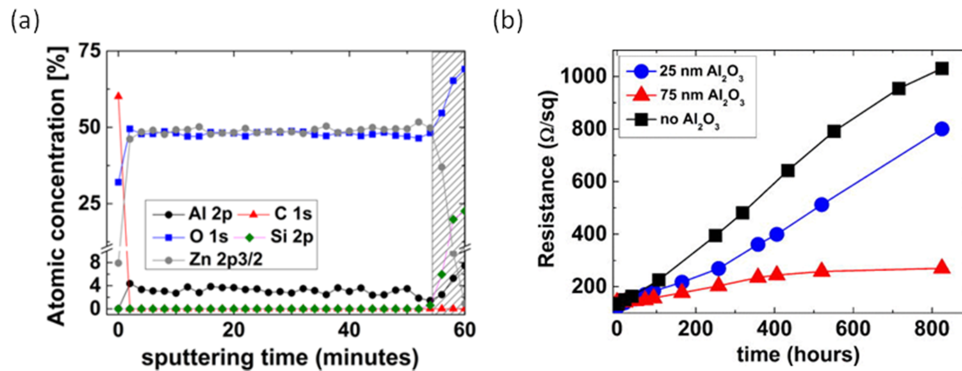

FIG. 8. (a) Composition of Al-doped ZnO measured by depth profiling XPS. Reprinted with permission from A. Illiberi, R. Scherpenborg, Y. Wu, F. Roozeboom, and P. Poodt, ACS Appl. Mater. Interfaces **5**, 13124 (2013). Copyright 2013 American Chemical Society. (b) Lifetime test of In-doped ZnO with and without a protective AP-SALD Al_2O_3 layer of 25 nm and 75 nm thickness, determined by measuring the change in sheet resistance of the films at 85 °C and 85% relative humidity. Reprinted with permission from A. Illiberi, R. Scherpenborg, M. Theelen, P. Poodt, and F. Roozeboom, J. Vac. Sci. Technol. A **31**, 061504 (2013). Copyright 2013 AIP Publishing LLC.

The co-injection method has been used for doping ZnO with Al by AP-SALD,[23] which can be challenging due to the high reactivity of the TMA precursor. This can result in the formation of a separate insulating alumina phase in the ZnO. Also, the optimum Al-content leading to the lowest resistivity is often very low (e.g., 8% Al/(Al + Zn) in AP-SALD Al-doped ZnO, or AZO).[27] This means that the amount of the Al precursor pre-mixed with the Zn-metal precursor gas flow needs to be reproducibly controlled to a very low value (e.g., <10 μmol min^{-1} bubbling rate through the TMA precursor compared to 95 μmol min^{-1} through the DEZ).[27] The co-injection method is, nevertheless, successful, as can be seen from the uniform Al concentration in the XPS depth-profile shown in Fig. 8(a). The doping efficiency[27] for these AP-SALD AZO films (using TMA as the precursor) is up to 70%, indicating that 70% of the Al dopants introduced to ZnO donate a free carrier. This is significantly higher than the doping efficiency of AZO produced by conventional ALD (<15%) using delta-doping of Al_2O_3 between ZnO layers (concept illustrated in Fig. 1(a)), showing the significant advantage of the co-injection approach, where the Al and Zn precursors chemisorb at the same time, resulting in more effective and uniform Al incorporation into the ZnO lattice.[11,27]

Using TMA as the Al precursor for Al-doping ZnO has the disadvantage that it can etch some of the Zn species, which is thought to be due to the high precursor reactivity and lower formation enthalpy of Al_2O_3 than ZnO.[14] Using a different Al precursor with larger ligands, such as DMAI (Table II), results in no observed Zn etching, and AZO forms solely by competitive chemisorption of DMAI and DEZ.[14,61,62] In conventional ALD, changing the Al precursor from TMA to DMAI also results in a wider dispersion of the Al dopant, leading to the doping efficiency increasing from 10% to 60%.[61] This is a similar doping efficiency as AP-SALD AZO made using the co-injection method,[27] further indicating that this method is successful in producing a uniform distribution of the dopant in ZnO films. The co-injection method used in AP-SALD has also been found to be effective in In-doping of ZnO. A resistivity decrease of three orders of magnitude resulted and a doping efficiency of 95% was obtained (Table II), which is comparable to that obtained by other techniques, such as sputtering.[29] As with AP-SALD AZO, In-doped ZnO has a high transparency of 90%, making this material highly suitable for TCOs. However, a major limitation to the industrial application of any ZnO-based material is that the resistivity increases in hot, humid environments due to structural degradation.[60] This has been overcome by covering the ZnO with a transparent AP-SALD Al_2O_3 layer (Fig. 8(b)), which acts as a stable moisture diffusion barrier.[60]

The rapid cycle times accessible to AP-SALD make selective area deposition particularly effective. This is because faster cycles reduce the likelihood of the precursors diffusing into the inhibitor. Much thicker films can thus be grown before unwanted growth in the masked areas occurs.[40] Such an approach lends itself to building circuits, since the active materials are deposited additively,

This article is copyrighted as indicated in the article. Reuse of AIP content is subject to the terms at: http://aplmaterials.aip.org/about/rights_and_permissions Downloaded to IP: 131.111.184.102 On: Mon, 01 Jun 2015 10:48:06

thus requiring no etching steps.[40] In Fig. 7(b), selective area deposition is demonstrated with AZO, where a 100 nm thick layer of AP-SALD AZO is deposited over the entire substrate. The precursor gases chemisorb only onto the areas without the poly(vinyl pyrrolidone) or PVP.[20,40] In this patterning approach, a polymeric inhibitor, such as PVP is printed, and the metal oxide films do not grow where the polymer coats the substrate.[20,40]

In summary, ZnO (intrinsic and doped) produced by AP-SALD has similar properties to films produced by conventional ALD. However, the important differences that make AP-SALD highly appealing are the higher growth rate (nm s^{-1}) due to faster cycling, atmospheric deposition that allows heat-sensitive substrates (e.g., organometal halide perovskites) to be loaded with minimal heating time, and compatibility with large area substrates and selective area deposition for rapid synthesis of electronics. In addition, the co-injection method employed in AP-SALD systems has the advantage of more uniform doping and high doping efficiency. This is particularly important for producing TCOs and for bandgap engineering via doping.

IV. OUTLOOK

The AP-SALD reactors that have mainly been used to study intrinsic and doped ZnO films are proof-of-principle and operate as batch processes for depositing materials onto single substrates. While industry versions of these reactors have the advantages of operating sheet-to-sheet and in-line with other processes,[6] fully realizing the high throughput potential of AP-SALD will likely require R2R processing.[5] Prototypes of these reactors have started to appear,[34,43,47] mainly for Al_2O_3 deposition. The knowledge generated on AP-SALD ZnO (intrinsic and doped) using the reactors shown in Sec. II can be applied to these new R2R reactors. A significant advantage of AP-SALD is that it combines the advantages of conventional ALD films (e.g., compact, high quality metal oxides) with also being compatible with R2R processing. Hence, AP-SALD is significantly advantageous over existing R2R techniques, such as slot-die coating.[23]

New dopants and higher-order multicomponent metal oxides based on ZnO should also be developed in the future. For example, amorphous indium gallium zinc oxide (IGZO) is appealing for high-volume TFT-display manufacturing, since it yields a tenfold higher electron mobility than amorphous silicon, in addition to improved performance even when fabricated at room temperature.[63,64] A very recent publication on the synthesis IGZO by AP-SALD is covered in Ref. 64. Yet, when depositing higher-order multicomponent metal oxides, the co-injection method of producing doped ZnO may be challenging if, for example, one distinct precursor has a much higher reactivity or vapor pressure than the other. Designing new, dedicated chemical precursors to tune these properties or introducing each precursor to a different gas channel is an option for overcoming this limitation. Anionic dopants for ZnO other than N should also be investigated, such as for Zn(O,S) (using H_2S as the sulfur source) to produce buffer layers in solar cells. Zn(O,S) has been deposited by pulsed-CVD to achieve high efficiencies in SnS solar cells.[65] AP-SALD Zn(O,S) has also very recently been synthesized and tested for CIGS (copper indium gallium selenide) solar cells.[66]

The device application fields of AP-SALD ZnO are currently mainly in the area of solar cells and TFTs, with Ref. 39 being the first report on the use of AP-SALD ZnO for LEDs and organometal halide perovskites. This opens up the possibility of applying the developments in the solar cell field to the fields of LEDs and organometal halide perovskite optoelectronics.[39,46] The low deposition temperatures and possibilities of coating large areas with ZnO and other metal oxides also give AP-SALD great promise for the paper electronics area.[67]

V. CONCLUSIONS

Mass production of ZnO by AP-SALD is highly appealing due to its scalability and the ability to control the electronic properties through doping. This has led to record performance improvements in solar cells and TFTs. Given its strong advantages, we expect AP-SALD to become as popular in laboratories as conventional ALD, which will spur the development of tailor-made chemicals for introducing dedicated doping of ZnO, as well as the production of multicomponent metal

This article is copyrighted as indicated in the article. Reuse of AIP content is subject to the terms at: http://aplmaterials.aip.org/about/rights_and_permissions
Downloaded to IP: 131.111.184.102 On: Mon, 01 Jun 2015 10:48:06

oxides. The key development with AP-SALD is to continue with the evolution to roll-to-roll reactors, necessary for production on a scale that fundamentally cannot be achieved with conventional ALD, as well as broadening the range of applications to encompass LEDs and organometal halide perovskite optoelectronics.

The authors acknowledge the support of the Rutherford Foundation of New Zealand and the Cambridge Commonwealth, European and International Trusts, and the ERC Advanced Investigator Grant, Novox, ERC-2009-adG247276. DMR acknowledges Marie Curie Actions (FP7/2007-2013, Grant Agreement Nos. 219332 and 631111), and the Ramon y Cajal 2011 programme from the Spanish MICINN and the European Social Fund, and the Comissionat per a Universitats I Recerca (CUR) del DIUE de la Generalitat de Catalunya, Spain.

[1] S. Strupp, Chem. Rev. **105**, 1023 (2005).
[2] ITRS 2013 Edition International Technology Roadmap for Semiconductors, 8 April 2014, http://www.itrs.net (14 April 2015).
[3] I. L. Markov, Nature **512**, 147 (2014).
[4] G. Fiori, F. Bonaccorso, G. Iannaccone, T. Palacios, D. Neumaier, A. Seabaugh, S. K. Banerjee, and L. Colombo, Nat. Nanotechnol. **9**, 768 (2014).
[5] D. Muñoz-Rojas and J. MacManus-Driscoll, Mater. Horiz. **1**, 314 (2014).
[6] P. Poodt, D. C. Cameron, E. Dickey, S. M. George, V. Kuznetsov, G. N. Parsons, F. Roozeboom, G. Sundaram, and A. Vermeer, J. Vac. Sci. Technol. A **30**, 010802 (2012).
[7] R. L. Z. Hoye, R. E. Brandt, Y. Ievskaya, S. Heffernan, K. P. Musselman, T. Buonassisi, and J. L. MacManus-Driscoll, APL Mater. **3**, 020901 (2015).
[8] S. M. George, Chem. Rev. **110**, 111 (2010).
[9] S. F. Nelson, D. H. Levy, L. W. Tutt, and M. Burberry, J. Vac. Sci. Technol. A **30**, 01A154 (2012).
[10] S. W. Lee, Y. S. Lee, J. Heo, S. C. Siah, D. Chua, R. E. Brandt, S. B. Kim, J. P. Mailoa, T. Buonassisi, and R. G. Gordon, Adv. Energy Mater. **4**, 1301916 (2014).
[11] Y. S. Lee, J. Heo, S. C. Siah, J. P. Mailoa, R. E. Brandt, S. B. Kim, R. G. Gordon, and T. Buonassisi, Energy Environ. Sci. **6**, 2112 (2013).
[12] M. Leskelä and M. Ritala, Angew. Chem., Int. Ed. **42**, 5548 (2003).
[13] T. Tynell and M. Karppinen, Semicond. Sci. Technol. **29**, 043001 (2014).
[14] A. Illiberi, P. Poodt, P.-J. Bolt, and F. Roozeboom, Chem. Vap. Deposition **20**, 234 (2014).
[15] T. Torndahl, C. Platzer-Bjorkman, J. Kessler, and M. Edoff, Prog. Photovoltaics: Res. Appl. **15**, 225 (2007).
[16] D. H. Levy, D. Freeman, S. F. Nelson, P. J. Cowdery-Corvan, and L. M. Irving, Appl. Phys. Lett. **92**, 192101 (2008).
[17] F. C. Krebs, Org. Electron. **10**, 761 (2009).
[18] Y. Ievskaya, R. L. Z. Hoye, A. Sadhanala, K. P. Musselman, and J. L. MacManus-Driscoll, Sol. Energy Mater. Sol. Cells **135**, 43 (2015).
[19] R. L. Z. Hoye, K. P. Musselman, and J. L. MacManus-Driscoll, APL Mater. **1**, 060701 (2013).
[20] D. H. Levy and S. F. Nelson, J. Vac. Sci. Technol. A **30**, 018501 (2012).
[21] L. Schmidt-Mende and J. L. MacManus-Driscoll, Mater. Today **10**, 40 (2007).
[22] D. C. Iza, D. Muñoz-Rojas, K. P. Musselman, J. Weickert, A. C. Jakowetz, H. Sun, X. Ren, R. L. Z. Hoye, J. H. Lee, H. Wang, L. Schmidt-Mende, and J. L. MacManus-Driscoll, Nanoscale Res. Lett. **8**, 359 (2013).
[23] R. L. Z. Hoye, D. Muñoz-Rojas, D. C. Iza, K. P. Musselman, and J. L. MacManus-Driscoll, Sol. Energy Mater. Sol. Cells **116**, 197 (2013).
[24] D. Muñoz-Rojas, H. Sun, D. C. Iza, J. Weickert, L. Chen, H. Wang, L. Schmidt-Mende, and J. L. Macmanus-Driscoll, Prog. Photovoltaics: Res. Appl. **21**, 393 (2013).
[25] R. L. Z. Hoye, B. Ehrler, M. L. Böhm, D. Muñoz-Rojas, R. M. Altamimi, A. Y. Alyamani, Y. Vaynzof, A. Sadhanala, G. Ercolano, N. C. Greenham, R. H. Friend, J. L. MacManus-Driscoll, and K. P. Musselman, Adv. Energy Mater. **4**, 1301544 (2014).
[26] B. Ehrler, K. P. Musselman, M. L. Böhm, F. S. F. Morgenstern, Y. Vaynzof, B. J. Walker, J. L. MacManus-Driscoll, and N. C. Greenham, ACS Nano **7**, 4210 (2013).
[27] A. Illiberi, R. Scherpenborg, Y. Wu, F. Roozeboom, and P. Poodt, ACS Appl. Mater. Interfaces **5**, 13124 (2013).
[28] R. L. Z. Hoye, S. Heffernan, Y. Ievskaya, A. Sadhanala, A. Flewitt, R. H. Friend, J. L. MacManus-Driscoll, and K. P. Musselman, ACS Appl. Mater. Interfaces **6**, 22192 (2014).
[29] A. Illiberi, R. Scherpenborg, F. Roozeboom, and P. Poodt, ECS J. Solid State Sci. Technol. **3**, P111 (2014).
[30] A. Illiberi, F. Roozeboom, and P. Poodt, ACS Appl. Mater. Interfaces **4**, 268 (2012).
[31] D. H. Levy, S. F. Nelson, and D. Freeman, J. Disp. Technol. **5**, 484 (2009).
[32] P. Poodt, A. Lankhorst, F. Roozeboom, K. Spee, D. Maas, and A. Vermeer, Adv. Mater. **22**, 3564 (2010).
[33] Z. Duan, A. Du Pasquier, Y. Lu, Y. Xu, and E. Garfunkel, Sol. Energy Mater. Sol. Cells **96**, 292 (2012).
[34] K. Ali, K.-H. Choi, and N. M. Muhammad, Chem. Vap. Deposition **20**, 380 (2014).
[35] D. Muñoz-Rojas, M. Jordan, C. Yeoh, A. T. Marin, A. Kursumovic, L. A. Dunlop, D. C. Iza, A. Chen, H. Wang, and J. L. MacManus-Driscoll, AIP Adv. **2**, 042179 (2012).
[36] K. P. Musselman, S. Albert-Seifried, R. L. Z. Hoye, A. Sadhanala, D. Muñoz-Rojas, J. L. MacManus-Driscoll, and R. H. Friend, Adv. Funct. Mater. **24**, 3562 (2014).
[37] N. Espinosa, H. F. Dam, D. M. Tanenbaum, J. W. Andreasen, M. Jørgensen, and F. C. Krebs, Materials **4**, 169 (2011).
[38] F. C. Krebs, J. Fyenbo, and M. Jørgensen, J. Mater. Chem. **20**, 8994 (2010).

This article is copyrighted as indicated in the article. Reuse of AIP content is subject to the terms at: http://aplmaterials.aip.org/about/rights_and_permissions
Downloaded to IP: 131.111.184.102 On: Mon, 01 Jun 2015 10:48:06

[39] R. L. Z. Hoye, M. R. Chua, K. P. Musselman, G. Li, M.-L. Lai, Z.-K. Tan, N. C. Greenham, J. L. MacManus-Driscoll, and R. H. Friend, Adv. Mater. **27**, 1414 (2015).
[40] C. R. Ellinger and S. F. Nelson, Chem. Mater. **26**, 1514 (2014).
[41] P. Poodt, V. Tiba, F. Werner, J. Schmidt, A. Vermeer, and F. Roozeboom, J. Electrochem. Soc. **158**, H937 (2011).
[42] N. Nandakumar, B. Dielissen, D. Garcia-Alonso, Z. Liu, and W. M. M. Kessels, in Technical Proceedings of the 6th World Conference on Photovoltaic Energy Conversion, Kyoto, Japan, 23–27 November 2014, http://www.solaytec.com/publications.
[43] A. S. Yersak, Y. C. Lee, J. A. Spencer, and M. D. Groner, J. Vac. Sci. Technol. A **32**, 01A130 (2014).
[44] K. Tapily, D. Gu, H. Baumgart, G. Namkoong, D. Stegall, and A. A. Elmustafa, Semicond. Sci. Technol. **26**, 115005 (2011).
[45] J. Nelson, Mater. Today **14**, 462 (2011).
[46] M. A. Green, A. Ho-Baillie, and H. J. Snaith, Nat. Photonics **8**, 506 (2014).
[47] P. Poodt, R. Knaapen, A. Illiberi, F. Roozeboom, and A. van Asten, J. Vac. Sci. Technol. A **30**, 01A142 (2012).
[48] C.-J. Ku, Z. Duan, P. I. Reyes, Y. Lu, Y. Xu, C.-L. Hsueh, and E. Garfunkel, Appl. Phys. Lett. **98**, 123511 (2011).
[49] W. E. Howard, in *Thin-Film Transistors*, edited by C. R. Kagan and P. Andry (Taylor & Francis, New York, NY, 2009), Chap. 1, p. 1.
[50] Y. S. Lee, D. Chua, R. E. Brandt, S. C. Siah, J. V. Li, J. P. Mailoa, S. W. Lee, R. G. Gordon, and T. Buonassisi, Adv. Mater. **26**, 4704 (2014).
[51] L.-N. Bai, J.-S. Lian, and Q. Jiang, Chin. Phys. Lett. **28**, 117101 (2011).
[52] S. Choopun, R. D. Vispute, W. Yang, R. P. Sharma, T. Venkatesan, and H. Shen, Appl. Phys. Lett. **80**, 1529 (2002).
[53] J. Tang and E. H. Sargent, Adv. Mater. **23**, 12 (2011).
[54] A. G. Pattantyus-Abraham, I. J. Kramer, A. R. Barkhouse, X. Wang, G. Konstantatos, R. Debnath, L. Levina, I. Raabe, M. K. Nazeeruddin, M. Graetzel, and E. H. Sargent, ACS Nano **4**, 3374 (2010).
[55] C.-H. M. Chuang, P. R. Brown, V. Bulović, and M. G. Bawendi, Nat. Mater. **13**, 796 (2014).
[56] N. K. Patel, S. Cinà, and J. H. Burroughes, IEEE J. Sel. Top. Quantum Electron. **8**, 346 (2002).
[57] L. Dunlop, A. Kursumovic, and J. L. MacManus-Driscoll, Appl. Phys. Lett. **93**, 172111 (2008).
[58] S. J. Lim, J.-M. Kim, D. Kim, S. Kwon, J.-S. Park, and H. Kim, J. Electrochem. Soc. **157**, H214 (2010).
[59] C. Lee and J. Lim, J. Vac. Sci. Technol. A **24**, 1031 (2006).
[60] A. Illiberi, R. Scherpenborg, M. Theelen, P. Poodt, and F. Roozeboom, J. Vac. Sci. Technol. A **31**, 061504 (2013).
[61] Y. Wu, S. E. Potts, P. M. Hermkens, H. C. M. Knoops, F. Roozeboom, and W. M. M. Kessels, Chem. Mater. **25**, 4619 (2013).
[62] Y. Wu, P. M. Hermkens, B. W. H. van de Loo, H. C. M. Knoops, S. E. Potts, M. A. Verheijen, F. Roozeboom, and W. M. M. Kessels, J. Appl. Phys. **114**, 024308 (2013).
[63] T. Kamiya and H. Hosono, NPG Asia Mater. **2**, 15 (2010).
[64] A. Illiberi, B. Cobb, A. Sharma, T. Grehl, H. Brongersma, F. Roozeboom, G. Gelinck, and P. Poodt, ACS Appl. Mater. Interfaces **7**, 3671 (2015).
[65] P. Sinsermsuksakul, K. Hartman, S. Bok Kim, J. Heo, L. Sun, H. Hejin Park, R. Chakraborty, T. Buonassisi, and R. G. Gordon, Appl. Phys. Lett. **102**, 053901 (2013).
[66] A. Illiberi, in AVS 61st International Symposium and Exhibition, Balimore, MD, 9–14 November 2014, p. 25, http://www2.avs.org/symposium2014/ProgramBooks/ProgramBook_Complete.pdf.
[67] D. Tobjörk and R. Österbacka, Adv. Mater. **23**, 1935 (2011).

This article is copyrighted as indicated in the article. Reuse of AIP content is subject to the terms at: http://aplmaterials.aip.org/about/rights_and_permissions Downloaded to IP: 131.111.184.102 On: Mon, 01 Jun 2015 10:48:06